10000 times volume reduction for fluorescence correlation spectroscopy using nano-antennas

Laura C. Estrada,[1,3,*] Pedro F. Aramendía,[2,3] and Oscar E. Martínez[1,3]

[1]*Dpto. de Física. Fac. de Ciencias Exactas y Naturales, Universidad de Buenos Aires, 1428, Buenos Aires, Argentina.*
[2]*INQUIMAE and Departamento de Química Inorgánica, Analítica y Química Física. Fac. de Ciencias Exactas y Naturales, Universidad de Buenos Aires, 1428, Buenos Aires, Argentina.*
[3]*CONICET. Consejo Nacional de Investigaciones Científicas y Técnicas, Argentina.*
[*]*Corresponding author: lestrada@df.uba.ar*

Abstract: We present an experimental and theoretical study of a new scheme for Near-Field Fluorescence Correlation Spectroscopy that, using the field enhancement by optical nanoantennas, allows the reduction of the observation volume 4 orders of magnitude below the diffraction limit. This reduction can be used in two different ways: to increase the sample concentration and to improve the spatial resolution of the dynamics under study. Our experimental results using individual gold nanoparticles and a 150μM Rose Bengal solution in glycerol confirm the volume reduction.

OCIS codes: (180.2520) Fluorescence microscopy; (180.4243) Near-field microscopy; (240.6680) Surface plasmons; (300.6280) Spectroscopy, fluorescence and luminescence.

References and links

1. D. Magde, E. Elson, and W. W. Webb, "Thermodynamic fluctuations in a reacting system-measurement by fluorescence correlation spectroscopy," Phys. Rev. Lett. **29**, 705-708, (1972).
2. E. Bismuto, E. Gratton, and D. C. Lamb "Dynamics of ANS Binding to Tuna Apomyoglobin Measured with Fluorescence Correlation Spectroscopy," Biophys. J. **81**, 3510-3521 (2001).
3. L. Kastrup, H. Blom, C. Eggeling, and S. W. Hell, "Fluorescence Correlation Spectroscopy in Subdiffraction Focal Volumes," Phys. Rev. Lett. **94,** 178104 (2005).
4. T. A. Klar, S. Jakobs, M. Dyba, A. Egner, and S. W. Hell, "Fluorescence microscopy with diffraction resolution barrier broken by stimulated emission," Proc. Nat. Acad. Sci. **97,** 8206-8210 (2000).
5. H. Rigneault and P. Lenne, "Fluorescence correlation spectroscopy on a mirror," J. Opt. Soc. Am. B **20**, 2203-2214 (2003).
6. T. E. Starr and N. L. Thompson, "Total Internal Reflection with Fluorescence Correlation Spectroscopy: Combined Surface Reaction and Solution Diffusion," Biophys. J. **80**, 1575-1584 (2001).
7. M. F. García-Parajó, B. I. de Bakker, M. Koopman, A. Cambi, F. de Lange, C. G. Figdor, and N. F. van Hulst, "Near-Field Fluorescence Microscopy: An optical Nanotool to Study Protein Organization at the Cell Membrane," NanoBiotechnology **1**, 113-120 (2005).
8. Y. Kawata, C. Xu, and W. Denk, "Feasibility of molecular-resolution fluorescence near-field microscopy using multi-photon absorption and field enhancenment near a sharp tip," J. Appl. Phys. **85**, 1294 (1999).
9. N. Calander, P. Muthu, Z. Gryczynski, I. Gryczynski, and J. Borejdo "Fluorescence correlation spectroscopy in a reverse Kretchmann surface plasmon assisted microscope," Opt. Express **16**, 13381-13390 (2008), http://www.opticsinfobase.org/abstract.cfm?URI=oe-16-17-13381.
10. J. Borejdo, N. Calander, Z. Gryczynski, and I. Gryczynski, "Fluorescence correlation spectroscopy in surface plasmon coupled emission microscope," Opt. Express **14**, 7878-7888 (2006), http://www.opticsinfobase.org/abstract.cfm?URI=oe-14-17-7878.
11. M. Foquet, J. Korlach, W. R. Zipfel, W. W. Webb, and H. G. Craighead, "Focal Volume Confinement by Submicrometer-Sized Fluidic Channels," Anal. Chem. **76**, 1618 – 1626 (2004).
12. M. J. Levene, J. Korlach, S. W. Turner, M. Foquet, H. G. Craighead, and W. W. Webb, "Zero-Mode Waveguides for Single-Molecule Analysis at High Concentrations," Science **299,** 682-686 (2003).
13. M. Leutenegger, M. Gösch, A. Perentes, P. Hoffmann, O. J. F. Martin, and T. Lasser, "Confining the sampling volume for Fluorescence Correlation Spectroscopy using a sub-wavelength sized aperture," Opt. Express **14**, 956-969 (2006), http://www.opticsinfobase.org/abstract.cfm?URI=oe-14-2-956.
14. J. Wenger, D. Gérard, P. Lenne, H. Rigneault, J. Dintinger, T. W. Ebbesen, A. Boned, F. Conchonaud, and D. Marguet, "Dual-color fluorescence cross-correlation spectroscopy in a single nanoaperture : towards rapid multicomponent screening at high concentrations," Opt. Express **14**, 12206-12216 (2006), http://www.opticsinfobase.org/abstract.cfm?URI=oe-14-25-12206.

#102665 - $15.00 USD Received 10 Oct 2008; revised 4 Nov 2008; accepted 4 Nov 2008; published 26 Nov 2008

15. H. Rigneault, J. Capoulade, J. Dintinger, J. Wenger, N. Bonod, E. Popov, T. W. Ebbesen, and P. F. Lenne, "Enhancement of Single-Molecule Fluorescence Detection in Subwavelength Apertures," Phys. Rev. Lett. **95**, 117401 (2005).
16. C. Zander, J. Enderlein, R. A. Keller (ed), *Single-Molecule Detection in Solution-Methods and Applications* (Wiley-VCH, 2002), Chap. 3.
17. C. Fradin, A. Abu-Arish, R. Granek, and M. Elbaum, "Fluorescence Correlation Spectroscopy Close to a Fluctuating Membrane," Biophys. J. **84**, 2005-2020 (2003).
18. L. Novotny and B. Hecht, *Principles of Nano-Optics* (Cambridge University Press, 2007).
19. F. Tam, G. P. Goodrich, B. R. Johnson, and N. J. Halas, "Plasmonic Enhancement of Molecular Fluorescence," Nano Lett. **7**, 496-501 (2007).
20. K. Aslan, I. Gryczynski, J. Malicka, E. Matveeva, J. R. Lakowicz, and C. D. Geddes, "Metal-enhanced fluorescence: an emerging tool in biotechnology," Curr. Op. in Biotech **16**, 55-62, (2005).
21. O. L. Muskens, V. Giannini, J. A. Sánchez-Gil, and J. Gómez Rivas, "Strong Enhancement of the Radiative Decay Rate of Emitters by Single Plasmonic Nanoantennas," Nano Lett. **7**, 2871-2875 (2007).
22. P. Anger, P. Bharadwaj, and L. Novotny, "Enhancement and Quenching of Single-Molecule Fluorescence," Phys. Rev. Lett. **96**, 113002, (2006).
23. P. Bharadwaj and L. Novotny, "Spectral dependence of single molecule fluorescence enhancement," Opt. Express **15**, 14266-14274 (2007), http://www.opticsinfobase.org/abstract.cfm?URI=oe-15-21-14266.

1. Introduction

Because of its high sensitivity, Fluorescence Correlation Spectroscopy (FCS) has become a very attractive and widespread tool that reaches single molecule sensitivity in studies of biological processes on a subcellular level. First introduced in the early 70´s by Magde, Elson and Webb [1], FCS measures the fluctuations of emission of single or few fluorescent molecules in the focal volume of a confocal or multiphoton microscope. In fluid media, the fluctuations are caused by diffusion, by photophysical processes or by any change in the mobility, that affects the transit time through the excitation volume (e.g. binding) [2]. Normally, it is useful only below ~100nM due to the limitations imposed by diffraction in reducing the observation volume. Cellular environments are most often excluded by this condition. Recently a number of different technologies have been introduced to reduce the detection volume a factor between 10 and 100 below the diffraction limit. They use optical phenomena such as stimulated emission depletion [3,4], and interference fringes in the excitation beam [5]. Other approaches rely on the use of near-field phenomena like total internal reflection [6], near-field fluorescence microscopy [7,8], and surface plasmon coupled emission [9,10], or mechanically confined compartments such as sub-microfluidic channels [11] or nanoholes [12-15].

In the present work, we describe a new scheme for Near-Field FCS which could be applied even inside a living cell. We show that it is possible to reduce a factor of 10^4 the observation volume in a controlled manner using the enhanced Far-Field to Near-Field (FF-NF) coupling by metallic nanoparticles (MNPs) upon surface plasmon excitation. We develop a theoretical expression for the autocorrelation function (ACF) based on the theory of correlation analysis for molecules diffusing near a spherical NP attached to a planar surface. We show that two parameters characterize the autocorrelation curve for a single chemical species: a transit time through the reduced observation volume τ_{small} and an amplitude β, which depends on the number of molecules in the confocal and in the reduced volumes, $<N_{large}>$, $<N_{small}>$, respectively, and on the intensity enhancement factor, α.

The volume reduction is visualized by comparing FCS experiments in its traditional and Near-Field forms using 150μM Rose Bengal solution in glycerol. As shown in Fig. 1(a), we use a spherical gold NP attached to a coverslip as an optical antenna. Although a spherical particle is not the most efficient antenna it has a geometry that makes the theoretical modeling of the system less complicated and a very reproducible shape for sample preparation, and in principle it can be applied to cell biology to analyze membrane and intracellular processes.

#102665 - $15.00 USD Received 10 Oct 2008; revised 4 Nov 2008; accepted 4 Nov 2008; published 26 Nov 2008

2. Theory

FCS, based on the measurement of equilibrium fluctuations, is quantified by the normalized auto-correlation function (ACF) of the detected fluorescence intensity at time t, I(t):

$$G(\tau)=\langle I(t)\cdot I(t+\tau)\rangle\big/\langle I\rangle^{2} \tag{1}$$

where τ is a lag time and the brackets represent time average. As shown in [16], for one single fluorophore freely diffusing in solution, the analytical expression of the ACF can be derived assuming a detected intensity of the form

$$I(r,t)=\int_{-\infty}^{+\infty} Q(r)\cdot p(r)\cdot C(r,t)dV \tag{2}$$

Where, *p(r)* defines the spatial dependence of brightness at which a molecule is seen by the detector and can be assumed in a confocal microscope to be Gaussian distributed in the axial and radial directions with rotation symmetry around the beam propagation direction. Q(r) is the product of the excitation cross-section of the molecule under study, its quantum yield, and the detection efficiency. C(r,t) is the molecule concentration at position *r* and at time *t*.

The situation encountered in our experiments is described in Fig. 1(a). The glass-liquid interface cuts the beam at the waist, and the spherical NP is located adjacent to the glass surface. A planar interface within the observation volume modifies the ACF. As the observation volume approaches and touches the interface (i. e. the coverslip), part of this volume becomes inaccesible to the fluorescent particles, the average number of fluorophores in the observation volume decreases, increasing in the amplitude of the ACF. This volume reduction also affects the average residence time of a fluorescent particle in the volume [17]. Besides these facts two distinct regions appear when the field distribution is considered. One is the large volume defined by the diffracting focussed beam and the confocal detection (region I in Fig. 1(a)). The second one is the region adjacent to the particle in the direction of polarization of the incoming electric field (regions II and III in Fig. 1(a)), where the field is enhanced due to the polarization induced in the NP. This region is about 1/10 of the particle diameter in thickness and about the NP diameter in width (symmetric respect to the polarization axis *x*). Free diffusing fluorescent molecules are reinjected in the observation volume after bouncing the glass and/or the particle surfaces. Three distinct bounces can be described, as illustrated in Fig. 1(b).

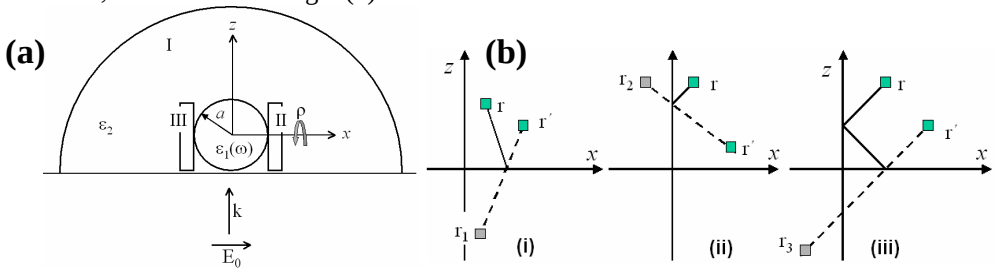

Fig. 1.(a): Scheme of the Near-Field FCS experiment. A NP is laying on a glass-liquid interface. (b): Considering a probe diffusing from r to r′, (i) reflected on the coverslip as coming from r_1, (ii) reflected on the NP as coming from r_2, (iii) reflected on both surfaces as coming from r_3.

Figure 2 (points) shows two calculated intensity profiles of the electric field in the vicinity of the NP using Mie theory as in [18]. In solid lines, Fig. 2 also shows that the intensity profiles can be very well approximated, in the range of distance of interest, by an exponential function of d = 8 nm in coordinate *x* and by a gaussian function of ω_0 = 33 nm in coordinate ρ for a gold NP of 40 nm radius. These approximations are essential to obtain an analytical integration of the total light intensity distribution Eq. (2) and hence for the total ACF. Due to the interaction with a metallic structure, fluorescence enhancement has been observed in several experiments [19-21]. This effect is the basis of the technique presented in this paper.

#102665 - $15.00 USD Received 10 Oct 2008; revised 4 Nov 2008; accepted 4 Nov 2008; published 26 Nov 2008

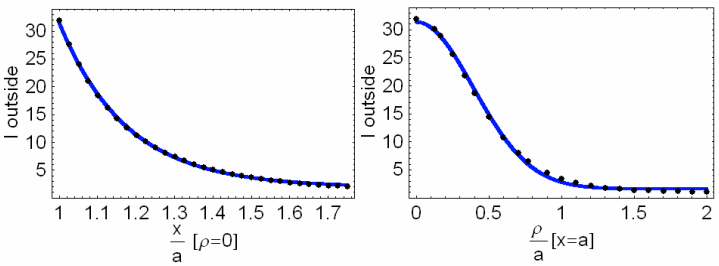

Fig. 2. Intensity profiles outside a spherical gold NP (distance is normalized to the radius *a* of the NP). Dots: Calculated according to Mie theory. Full line: Fits to exp(-x/d) (left) and $\exp[-2\rho^2/\omega_0^2]$ (right). Both d and ω_0 scale linearly with the particle radius *a*.

In the experiment, Fig. 1(a), fluorescent molecules are in close proximity to MNPs. It is well known that in this situation, the local electric field enhancement leads to an increase in the excitation rate whereas non radiative energy transfer to the NP leads to a decrease in the molecule quantum yield, ϕ, relative to ϕ_0, where the subscript "0" indicates the value in the absence of a NP. The results of these two effects have been studied in detail [22,23]. Anger and co-workers [22] show the fluorescence rate of a single molecule as a function of its distance to a MNP. In the referenced work, ϕ_0 was set to 1 for calculations but in our case we are interested in exploring this dependence for molecules with $\phi_0 << 1$.

Our calculations showed very interesting features not explored in detail before. For very small MNP-molecule distance (less than 1nm), there is a quenching effect, as reported previously [22,23], beyond this distance there is a region of sharp enhancement, whose extension depends on the orientation of molecules under study, and very strongly on ϕ_0. The interaction of the excited molecule with the NP opens an energy transfer channel that results in excited state lifetime shortening and enhanced emission rate provided by this energy transfer mechanism. As a consequence, the fluorescence enhancement increases with the decrease in the quantum yield of the molecule in the absence of NP, ϕ_0, from a value of 1.75 for $\phi_0 = 1$ to 70 for $\phi_0 = 0.01$. The NP captures the energy from the near field of the molecule and couples it to the far field through the resonant plasmon excitation (nanoantenna effect). We conclude that, for weakly fluorescent molecules, we reach a tremendous enhancement but, more important, we improve the contrast between the enhanced and not enhanced regions, restricting the zone of detection and allowing the determination of small changes in the number of even very weakly fluorescent molecules.

An analytical solution for the ACF is found for molecules diffusing in a 3D-Gaussian volume with the addition of one MNP at the center of the observation volume. We take into account the distribution and the enhancement of the electric field near the NP, as well as the presence of a planar interface within the observation volume as in [17]. To describe the field near the NP we use the approximations studied in Fig. 2. With these assumptions the total spatial dependence of brightness, $p_T(r)$ of Eq. (2), is simply obtained by

$$p_T(r) = p_{3DG}(r) + \alpha \cdot p_{2DG-\exp}(r) \tag{3}$$

The term $p_{3DG}(r)$ (3D Gaussian) gives the detected profile in absence of the NP and is the same as in the case of free diffusion [16]. The term $p_{2DG\text{-}exp}(r)$ is a consequence of the presence of the NP, and α the intensity enhancement factor. With some simplifications (see Appendix for details) the integrations in Eq. (2) for the case of diffusion can be written as

$$G_{diff}(\tau) = \frac{32}{\langle N_{large}\rangle^2}\alpha^2 \frac{\langle N_{small}\rangle}{2(4\tau/9\tau_{small}+1)}\left(\frac{2}{\sqrt{\pi}}\sqrt{\frac{\tau}{\tau_{small}}} + e^{\frac{\tau}{\tau_{small}}}\left(1-2\frac{\tau}{\tau_{small}}\right)Erfc\left[\sqrt{\frac{\tau}{\tau_{small}}}\right]\right) \tag{4}$$

Here, $\langle N_i \rangle$ is the mean number of molecules in volume *i* defined by $V_{small} = \pi\omega_0^2 d$ and $V_{large} = \pi^{3/2}\omega_{01}^2\omega_z$ and the residence time is $\tau_{small} = d^2/D$, where D is the diffusion coefficient.

#102665 - $15.00 USD Received 10 Oct 2008; revised 4 Nov 2008; accepted 4 Nov 2008; published 26 Nov 2008

3. Experimental results

We used a commercial confocal microscope FV1000 from Olympus Inc. Fluorescent molecules were excited with a 543nm linearly polarized laser beam. Intensity variations of the fluorescent signal were detected with a photomultiplier in single photon counting mode and processed with a software correlator (SimFCS, software developed at the LFD, Illinois). Commercial gold NPs (from Ted Pella, USA) were attached onto a polyethylenimine (PEI)-functionalized coverslip to give a coverage of ~0.1 particles/μm^2. A drop of 150μM Rose Bengal (Aldrich) in 80% glycerol/water (Fluka) solution was used as the fluorescent sample.

The confocal observation volume was determined by a calibration experiment. Afterwards, a transmission image was taken to identify the position of the NPs. Because the position and shape of the plasmon absorption of MNPs are strongly dependent on the size and particle material, the extinction spectrum of a single NP was measured to ensure the presence of gold. Finally the fluorescence signal as a function of time was recorded either over a NP or over a region without NPs. We observe correlation at 150μM dye concentration, 10^4 times the concentrations used in standard experiments.

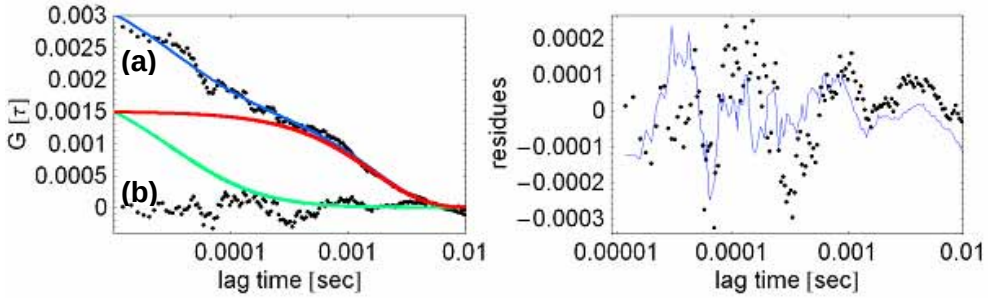

Fig. 3. (Left): ACF for 150μM Rose Bengal in 80% glycerol/water at room temperature acquired with (a), and without (b) a 40nm radius gold NP in the observation volume. The fit of the experimental data with Eq. (5) and the individual contributions of each process (diffusion in green and binding kinetics in red) to the total ACF are also shown. (Right): Comparison of the residuals obtained by fitting the experimental data with Eq. (5) (solid line), and the correlation without a NP (background signal), curve (b) of left panel (points).

Results are summarized in Fig. 3, which clearly indicates that a non-correlated signal changes to a correlated one when a NP is present within the excitation volume, confirming the volume reduction. All measurements show two characteristics times. The fast component has a characteristic time in the μs range, while the slow one falls in the ms range. In all the cases we found that a diffusion model with binding dynamics, Eq. (5), fits the results very well.

$$G_T(\tau)=\beta\frac{1}{(4\tau/9\tau_{small}+1)}\left(\frac{2}{\sqrt{\pi}}\sqrt{\frac{\tau}{\tau_{small}}}+e^{\frac{\tau}{\tau_{small}}}\left(1-2\frac{\tau}{\tau_{small}}\right)Erfc\left[\sqrt{\frac{\tau}{\tau_{small}}}\right]\right)+Ae^{-\frac{\tau}{\tau_R}} \quad (5)$$

Equation (5) has four adjustable parameters, two amplitudes: β and A; and two characteristic times: τ_{small} and τ_R. The fast component, τ_{small} is consistent with the diffusion through the enhanced volume V_{small}, and the slow component, τ_R suggests a binding-unbinding interaction between the molecule and the NP surface. *A* is the fraction of molecules being in a bound state and $\beta = 16\alpha^2 \langle N_{small} \rangle / \langle N_{large} \rangle^2$ is a combination between the intensity enhancement factor and the volumes ratios. This result shows the ability to study not only the diffusion behavior of molecules, but also the interaction with the NP surface. The individual contributions of each process to the total ACF are also shown in Fig. 3. Excellent agreement to the experimental curve is obtained with $\beta = 0.0021$, $A = 0.0015$, $\tau_{small} = 27\mu sec$ and $\tau_R = 1.6msec$.

4. Conclusions

We have shown theoretically and experimentally that using the enhanced FF-NF coupling by MNPs alows to reduce the observation volume 4 orders of magnitude. This reduction can be

#102665 - $15.00 USD Received 10 Oct 2008; revised 4 Nov 2008; accepted 4 Nov 2008; published 26 Nov 2008

used in two different ways, *i)* to increase the sample concentration, and *ii)* to improve the spatial resolution of the dynamics under study. Experiments performed at 0.1mM open potential applications of FCS to explore subcellular environments with a great spatial resolution and still measure mobility using the intrinsic fluorescence of very weakly emitting molecules.

Appendix: Derivation of the ACF

In its most general form the ACF is defined as

$$G(\tau)=\int_V\int_{V'} Q^2(r)\cdot p_T(r)\cdot p_T(r')\cdot g(r,r',\tau)dVdV' \Big/ \left(\langle c\rangle \int_V Q(r)\cdot p(r)dV\right)^2 \quad \text{(A1)}$$

where $g(r,r',\tau)=\langle \delta C(r,t)\delta C(r',t+\tau)\rangle$ can be calculated using Fourier transforms in the spatial domain. Because $p_T(r)$ can be obtain by the superposition of two terms (see text) $p_T(r)=p_1(r)+\alpha\cdot p_2(r)$, the ACF can be expressed as the sum of 4 terms:

$$G_{ij}(\tau)=\kappa\int_V\int_{V'} Q^2(r)\cdot p_i(r)\cdot p_j(r')\cdot g(r,r',\tau)dVdV' \Big/ \left(\langle c\rangle \int_V Q(r)\cdot p_T(r)dV\right)^2 \quad \text{(A2)}$$

where κ is 1, 2α, 2α, $2\alpha^2$ for (i,j) = (1,1), (1,2), (2,1), (2,2) respectively, and where the factor two comes from the fact that $G_{12}(\tau) = G_{13}(\tau)$; $G_{21}(\tau) = G_{31}(\tau)$ and $G_{22}(\tau) = G_{33}(\tau)$;
Due to the presence of the NP we are assuming that there is no correlation between regions II and III, $G_{23}(\tau) = G_{32}(\tau) = 0$. Assuming Eq. (3) for $p_T(r)$, the complete ACF has 3 terms,

$$G(\tau)=\left[\frac{\langle N_{large}\rangle}{4\sqrt{2}}+\alpha\langle N_{small}\rangle\right]^{-2}\left(f_0+f_1+f_2\right) \quad \text{(A3)}$$

$$f_0=\frac{\langle N_{large}\rangle}{16}\left[\left(\tau/\tau_{large}\right)+1\right]^{-1}\left[\left(\tau/25\tau_{large}\right)+1\right]^{-1/2}$$

$$f_1=\alpha\frac{2\langle N_{small}\rangle}{\left(\frac{2\tau}{\tau_{large}}+1+\frac{\omega_{02}^2}{\omega_{01}^2}\right)^{1/2}\left(\frac{2\tau}{25\tau_{large}}+1+\frac{\omega_{02}^2}{25\omega_{01}^2}\right)^{1/2}}e^{-2a^2\Big/25\omega_{01}^2\left(\frac{2\tau}{25\tau_{large}}+1+\frac{\omega_{02}^2}{25\omega_{01}^2}\right)}$$

$$f_2=\alpha^2\frac{\langle N_{small}\rangle}{2\left(4\tau/9\tau_{small}+1\right)}\left(\frac{2}{\sqrt{\pi}}\sqrt{\frac{\tau}{\tau_{small}}}+e^{\frac{\tau}{\tau_{small}}}\left(1-2\frac{\tau}{\tau_{small}}\right)Erfc\left[\sqrt{\frac{\tau}{\tau_{small}}}\right]\right)$$

The term f_0 does not depend on α, and corresponds to the correlation between the confocal observation volume with itself. The term f_2, which is proportional to α^2, describes the concentration fluctuation within the reduced volume. Finally, the term in f_1 considers the probability to find a fluorophore in V_{large} at *t* if it was in V_{small} at *t = 0* and viceversa.
In the absence of a NP (α = 0) the only term that survives is f_0. As we did not observe any correlation without a NP (Fig. 3, curve (b)), this term can be neglected. Moreover, for realistic values of parameters, $f_1 < f_0$ and hence the only relevant term is f_2. Considering that the volume reduction is on the order of 10^4, for α<2000, $\langle N_{large}\rangle/4\sqrt{2} >> \alpha\langle N_{small}\rangle$. With all these assumptions we can approximate the ACF in the case of pure diffusion by Eq. (A4), which is Eq. (4) of the text.

$$G_{diff}(\tau)\approx 32\, f_2 \Big/ \langle N_{large}\rangle^2 \quad \text{(A4)}$$

#102665 - $15.00 USD Received 10 Oct 2008; revised 4 Nov 2008; accepted 4 Nov 2008; published 26 Nov 2008